THE JOURNAL OF BIOLOGICAL CHEMISTRY VOL. 285, NO. 2, pp. 1188–1198, January 8, 2010

Functional Consequences of Homocysteinylation of the Elastic Fiber Proteins Fibrillin-1 and Tropoelastin*

Received for publication, May 14, 2009, and in revised form, September 29, 2009 Published, JBC Papers in Press, November 4, 2009, DOI 10.1074/jbc.M109.021246

Dirk Hubmacher[‡], Judith T. Cirulis[§], Ming Miao[§], Fred W. Keeley[§], and Dieter P. Reinhardt[‡¶1]

From the [‡]Faculty of Medicine, Department of Anatomy and Cell Biology, and the [¶]Faculty of Dentistry, Division of Biomedical Sciences, McGill University, Montreal, Quebec H3A 2B2 and the [§]Research Institute, The Hospital for Sick Children, Toronto, Ontario M5G 1X8, Canada

Homocystinuria caused by cystathionine-β-synthase deficiency represents a severe form of homocysteinemias, which generally result in various degrees of elevated plasma homocysteine levels. Marfan syndrome is caused by mutations in fibrillin-1, which is one of the major constituents of connective tissue microfibrils. Despite the fundamentally different origins, both diseases share common clinical symptoms in the connective tissue such as long bone overgrowth, scoliosis, and ectopia lentis, whereas they differ in others. Fibrillin-1 contains ~13% cysteine residues and can be modified by homocysteine. We report here that homocysteinylation affects functional properties of fibrillin-1 and tropoelastin. We used recombinant fragments spanning the entire fibrillin-1 molecule to demonstrate that homocysteinylation, but not cysteinylation leads to abnormal self-interaction, which was attributed to a reduced amount of multimerization of the fibrillin-1 C terminus. The deposition of the fibrillin-1 network by human dermal fibroblasts was greatly reduced by homocysteine, but not by cysteine. Furthermore, homocysteinylation, but not cysteinylation of elastin-like polypeptides resulted in modified coacervation properties. In summary, the results provide new insights into pathogenetic mechanisms potentially involved in cystathionine-β-synthase-deficient homocystinuria.

Homocystinuria (OMIM +236200) and Marfan syndrome (OMIM #154700) share some common clinical symptoms such as ectopia lentis, long bone overgrowth, and scoliosis, but differ significantly in other symptoms. Marfan syndrome is caused by mutations in fibrillin-1, whereas homocystinuria is caused in most cases by cystathionine-β-synthase (CBS)[2] deficiency, an enzyme that converts homocysteine to cystathionine resulting in highly elevated homocysteine and methionine and reduced cysteine concentrations (1). In addition, various defects or polymorphisms in genes for the methionine and vitamin B_{12} metabolism result in elevated blood levels of homocysteine, ranging from 15 to 20 μM (mild forms) up to 500 μM (severe forms), compared with 5–10 μM under normal conditions (2–4).

Fibrillins belong to a family of modular extracellular matrix proteins including three isoforms, fibrillin-1, -2, and -3, and the latent transforming growth factor-β-binding proteins (for a recent review, see Ref. 5). The most abundant domains in fibrillins are characterized by 6–8 intra-domain disulfide bonds and include the calcium-binding epidermal growth factor-like (cbEGF) domain and the transforming growth factor-β binding protein-like domain. These domains represent individual folding units and are essential to maintain the structural integrity and functional properties of fibrillins (for review, see Ref. 6). The most common mutations reported to cause Marfan syndrome delete or generate cysteines in these domains, leading to the presence of at least one unpaired cysteine residue (7). Selected mutations of this group result in a modification of the secondary structure *in vitro*, rendering the molecules susceptible to proteolytic degradation (8, 9).

The functional entities of fibrillins in tissues are high molecular weight multiprotein assemblies, called microfibrils (10–12). Disulfide bond-mediated multimerization of the fibrillin-1 C terminus and N- to C-terminal self-interaction are thought to be the initial steps in the formation of tissue microfibrils (13–15). Microfibrils were suggested to serve as a scaffold for the deposition of tropoelastin and are important for the maintenance of elastic fibers in skin, lung, and aorta (16). This hypothesis has been further substantiated by the analysis of fibrillin-1 and -2 double null mice that show only traces of elastic fibers between smooth muscle cells in the developing aorta *versus* much more organized lamellar units visible in wild-type animals (17, 18). In addition to the role as a structural scaffold, microfibrils serve as a reservoir for growth factors such as transforming growth factor-β or bone morphogenetic proteins (19–22).

Elastic fibers are essential entities in skin, blood vessels, and lung, where they confer tissue elasticity. During elastic fiber biogenesis, monomeric tropoelastin forms small aggregates on the cell surface, which are deposited on the microfibril scaffold. After cross-linking and other maturation steps, they are transformed into a highly insoluble and mechanically durable material (18, 23). Tropoelastin contains two cysteine residues that are located in the conserved C terminus, where they form an intra-molecular disulfide bond (24). The self-assembly process for tropoelastin and the properties of elastin-like polypeptides can be experimentally assessed in a temperature-induced phase

* This work was supported by a grant from the Canadian Marfan Association (to D. P. R.), Canadian Institutes of Health Research Grant MOP-68836 (to D. P. R.), the German Academic Exchange Service (to D. H.), and Heart and Stroke Foundation of Ontario Grant T5451 (to F. W. K.).

[1] To whom correspondence should be addressed: 3640 University St., Montreal, QC H3A 2B2, Canada. Tel.: 514-398-4243; Fax: 514-398-5375; E-mail: dieter.reinhardt@mcgill.ca.

[2] The abbreviations used are: CBS, cystathionine-β-synthase; BSA, bovine serum albumin; cbEGF, calcium-binding epidermal growth factor-like domain; DMEM, Dulbecco's modified Eagle's medium; DTT, dithiothreitol; HSF, primary human skin fibroblasts; MES, 2-(*N*-morpholino)ethanesulfonic acid; PBS, phosphate-buffered saline; TBS, Tris-buffered saline.

separation, known as coacervation (25, 26). This process is dependent on factors such as ionic strength, pH, polypeptide concentration, and the presence of other extracellular matrix proteins (27–31).

The consequences of elevated homocysteine have been studied in a number of *in vivo* and cell culture models. In chick, high homocysteine levels resulted in a reduced amount of fibrillin-2 and microfibrils in the elastic lamina of the aorta (32). A defect in fibrillin-1 deposition by smooth muscle cells was mechanistically linked to a deficiency in cysteine rather than to elevated homocysteine levels (33). Baumbach *et al.* (34) showed that the structures of cerebral arterioles are altered in heterozygous $Cbs^{+/-}$ mice on a high methionine diet. These authors observed a hypertrophy of cerebral arterioles resulting from an increase in the cross-sectional area of the arteriolar wall, attributed to an increase in the ratio of smooth muscle cells and elastin components *versus* the stiffer components like collagen and basement membranes that remained constant. Recently, we and others showed that fragments of fibrillin-1 are a target for homocysteine (35, 36). The modified fragments became more susceptible to proteolysis, lost their ability to bind calcium, and demonstrated an altered secondary structure.

Here we demonstrate consequences of homocysteinylation on functional properties of fibrillin-1 and tropoelastin. Homocysteinylation of fibrillin-1 led to alterations of self-interaction properties. This was functionally attributed to a reduction of disulfide-bonded C-terminal fibrillin-1 multimers. In a cell culture model, the deposition of a fibrillin-1 network was reduced after incubation with homocysteine, but not with cysteine. Using elastin-like polypeptides, we demonstrate a functional consequence of homocysteinylation on the coacervation properties. These data provide new important insights in potential pathogenetic mechanisms leading to the connective tissue phenotype observed in individuals with homocystinuria caused by CBS deficiency.

EXPERIMENTAL PROCEDURES

Recombinant Fibrillin-1 Fragments and Elastin-like Polypeptides—The N-terminal (rFBN1-N) and C-terminal (rFBN1-C) halves of human fibrillin-1 were expressed with a hexahistidine tag at the C terminus in human embryonic kidney cells (293, American Type Culture Collection) and purified using Ni^{2+}-chelating chromatography as described previously (35, 37, 38). Separation of rFBN1-C multimers from monomers was performed by gel filtration chromatography as described in detail elsewhere (13). The purity of the proteins was assessed using SDS-PAGE under reducing conditions (20 mM dithiothreitol (DTT)). Proteins were stored in 50 mM Tris, 150 mM NaCl, pH 7.4 (TBS), including 2 mM $CaCl_2$.

Expression, purification, and characterization of the elastin-like polypeptide EP20-24-24 containing the protein sequence encoded by exons 20-21-23-24-21-23-24 of human tropoelastin has been described previously (27). The construct for expression of EP20-24-24/36, which includes additionally the protein sequence coded by exon 36 of human tropoelastin containing the two cysteine residues, was generated by a PCR strategy using the EP20-24-24 plasmid as template and the following primers representing exon 36 and additional restriction sites for cloning: BamHI-Ex20, 5′-CTGCTAGGGGGATCCATGTTTCCCGGCTTT-3′; Ex24/36-EcoRI, 5′-AGGGAATTCCTATTTTCTCTTCCGGCCACAAGCTTTCCCCAGGCAGGCCCCACCAGGGCCAATCGCGGGA-3′.

The corresponding PCR product (~650 bp) was purified, digested with restriction enzymes BamHI and EcoRI, and ligated into a BamHI/EcoRI-treated pGEX-2T expression vector (Amersham Biosciences). Primer synthesis and sequence confirmation were performed by The Centre for Applied Genomics at The Hospital for Sick Children. Expression and purification of the polypeptide used techniques described previously (27, 28). The identity of the polypeptide product was confirmed by amino acid analysis and mass spectrometry, both performed by the Advanced Protein Technology Center at The Hospital for Sick Children.

Preparation of Homocysteine and Homocysteinylation of Proteins—L-Homocysteine was prepared by reacting cyclic L-homocysteine-thiolactone (Sigma) with 5 M NaOH using an established procedure with minor modifications as described in detail elsewhere (35, 39). To prevent oxidation, aliquots were frozen immediately either on dry ice or in liquid nitrogen, stored at −80 °C, and re-thawed only once. The cysteine stock solution was prepared by dissolving L-cysteine hydrochloride (Fluka) in the same buffer as the final buffer after homocysteine preparation (150 mM NaOH, 150 mM KH_2PO_4, pH ~ 7). Aliquots were frozen and stored as described above for homocysteine. Homocysteine and cysteine used in cell culture assays was sterile filtrated (0.22 μm) before aliquotation. To determine the concentration of free thiol groups in homocysteine and cysteine solutions, Ellman reagent (5,5′-dithiobis 2-nitrobenzoic acid, Fisher Scientific) was used according to the manufacturer's protocol (40).

To simulate pathological conditions, fibrillin-1 fragments rFBN1-N and rFBN1-C were incubated with 0–1000 μM homocysteine or with cysteine as a control at 37 °C for 24–72 h. After 12 h, a second aliquot of homocysteine or cysteine was added to compensate for the relatively short half-life of homocysteine and cysteine due to oxidation. The proteins were dialyzed against TBS including 2 mM $CaCl_2$ and the concentration was determined using the BCA protein assay kit (Pierce). The integrity of the proteins was assessed using SDS-PAGE and Coomassie Brilliant Blue staining (G-250, Fisher Scientific). To control for acidification in thiol concentrations above 500 μM, 1 M Tris (pH 7.4) was added to a final concentration of 33.3 mM.

Solid Phase Binding Assays—The methodology for the solid phase binding assays was previously described (41). Briefly, 1 μg of protein/well in TBS was coated on a 96-well Maxisorp flat bottom plate (Nalge Nunc International) overnight at 4 °C. After blocking with 5% nonfat milk in TBS (blocking buffer), the soluble ligand was added in blocking buffer including 2 mM $CaCl_2$ either in 1:3 serial dilutions starting from 50 μg/ml, or in 1:2 serial dilutions starting from 100 μg/ml. Bound proteins were detected using a primary polyclonal rabbit antibody against rFBN1-N or rFBN1-C (1:1000 diluted in blocking buffer) (42, 43), and a secondary horseradish peroxidase-conjugated antibody (Peroxidase AffiniPure goat anti-rabbit IgG, 1:800, Jackson ImmunoResearch Laboratories Inc.). The color reaction was performed using 1 mg/ml of 5-aminosalicylic acid (Sigma) dissolved in 20 mM phosphate buffer (pH 6.8) including

0.045% (v/v) hydrogen peroxide. The reaction was stopped with 2 M NaOH and the absorbance at 492 nm was measured using a microplate reader (AD 340, Beckman Coulter). To compare different sets of experiments, relative binding values were calculated by setting the absolute binding at the highest soluble ligand concentration of the control to 100%. The curves were fitted using a hyperbolic model: $A_{492} = (P_1 \times [L])/(P_2 + [L])$ (Origin software version 7), where A_{492} represents the absorption at 492 nm, [L] the concentration of the soluble ligand in nM, P_1 the overall binding, and P_2 the dissociation constant (K_D) in nanomolar. Statistical significance was calculated employing the two-sided Student's *t* test. The solid phase binding assay technique using antibodies as the detection method has restrictions in deducing absolute values for binding affinities. This is due to the non-linearity of the detection signals generated by primary and secondary antibodies (44). Therefore, the binding data after hyperbolic curve fitting provide apparent values, which can be used to compare the effects of homocysteine and cysteine on fibrillin-1 interaction properties. The term "overall binding" refers to the value on the *y* axis obtained for the horizontal asymptote after hyperbolic curve fitting, and the term "apparent K_D" refers to the concentration of soluble ligand in nanomolar resulting in 50% overall binding. Note that the apparent K_D is reciprocal to the apparent affinity.

To immobilize heparin derived from porcine intestinal mucosa (Sigma; product number H3393) on a 96-well plate, it was covalently coupled to bovine serum albumin (BSA, Fisher Thermo Scientific, BP1605-100) using 1-ethyl-3-(3-dimethylaminopropyl)carbodiimide hydrochloride (Pierce) as a cross-linker. Aliquots of 0.2 ml of BSA (20 mg/ml in 0.1 M MES (pH 4.7)) were mixed with 0.5 ml of heparin sodium salt (10 mg/ml in 0.1 M MES, pH 4.7), added to 0.1 ml of 1-ethyl-3-(3-dimethylaminopropyl)carbodiimide hydrochloride (10 mg/ml in water) and incubated for 2 h at 22 °C in an Eppendorf shaker (900 rpm). To separate the cross-linked BSA-heparin from the non-reacted BSA and heparin, the reaction mixture was loaded on a Superose 12 gel filtration column (GE Healthcare), equilibrated in 0.1 M NaH_2PO_4, 900 mM NaCl (pH 7.2) at 0.5 ml/min. Fractions of 1 ml were collected and tested for reactivity with rFBN1-N and rFBN1-C by solid phase binding assay. Positive fractions were pooled, the protein concentration was determined using the BCA assay and stored at −20 °C.

Immunofluorescence—Primary human skin fibroblasts (HSFs) were isolated from the foreskins of healthy individuals (2–5 years of age) after a standard circumcision procedure. The procedure was approved by the local ethics committee (PED-06-054), and informed consent was obtained from the parents of the tissue donors. HSFs were used for the experiments between passages 2 and 7 and grown at 37 °C in a 5% CO_2 atmosphere with Dulbecco's modified Eagle's medium supplemented with 2 mM glutamine, 100 units/ml of penicillin, 100 μg/ml of streptomycin, and 10% fetal calf serum (DMEM; Wisent Inc.). For immunofluorescence experiments, cells were seeded in 8-well chamber slides (7.5×10^4 cells/well) and the medium was changed after 24 h to DMEM containing homocysteine or cysteine. For the next 3 days, the medium was changed every 12 h to mimic a "long term" exposure to homocysteine or cysteine. Following a washing step with phosphate-buffered saline (PBS; 137 mM NaCl, 2.7 mM KCl, 4.3 mM Na_2HPO_4, and 1.47 mM KH_2PO_4, pH 7.4, general washing buffer), the cells were fixed in ice-cold 70% methanol, 30% acetone. Cells were washed again, blocked for 60 min with PBS including 10% normal goat serum (PBS-G) (Jackson ImmunoResearch Laboratories, Inc.), and incubated with the primary anti-fibrillin-1 α-rFBN1-C (1:1000) and anti-fibronectin FN-15 (Sigma, 1:1000) diluted in PBS-G for 2 h. After washing, the cells were incubated for 2 h with fluorescein isothiocyanate-labeled goat anti-mouse (1:100) and Cy3-labeled goat anti-rabbit (1:200) secondary antibodies (Jackson ImmunoResearch Laboratories, Inc.) diluted in PBS-G. After washing with PBS and one wash with distilled water, the nuclei of the cells were stained with 4′-6-diamidino-2-phenylindole (1 μg/ml in distilled water; Invitrogen), washed again with water, coverslipped, and examined using an Axioskop 2 microscope, equipped with an Axiocam camera (Zeiss). Pictures were taken using AxioVision software version 3.1.2.1 (Zeiss).

Dot-blot Analysis of Secreted Extracellular Matrix Proteins—The secretion of fibrillin-1 and fibronectin from HSFs into the culture medium was monitored by dot-blot analysis. 25 μl of the medium of HSFs grown in the chamber slides for immunofluorescence experiments were diluted in 475 μl of TBS. The samples were blotted on a 0.45-μm nitrocellulose membrane (Bio-Rad) using a Bio-dot microfiltration apparatus (Bio-Rad). The membrane was blocked with TBS including 5% nonfat milk for 1 h, followed by a 2-h incubation with the primary α-rFBN1-C (1:1000) and FN-15 (1:1000) antibodies, diluted in 5% BSA in TBS. After a 2-h incubation with either goat anti-rabbit or goat anti-mouse horseradish peroxidase conjugate (both diluted 1:800 in TBS), the dot-blot was developed in TBS, 17% methanol, including 0.02% (v/v) H_2O_2 and 0.5 mg/ml of 4-chloro-1-naphthol.

Quantitative Real Time-Polymerase Chain Reaction—30×10^4 HSFs in DMEM were seeded on a 6-well plate (Costar, Corning Inc.) in duplicates and after 24 h, the medium was changed to DMEM including homocysteine or cysteine. The medium was changed every 12 h for 3 days. Total RNA was extracted using the RNeasy Plus Mini Kit (Qiagen) as instructed by the supplier. The same amounts of total RNA from each set of samples was reverse-transcribed with random hexamer primers and Superscript III (Invitrogen) using the manufacturer's protocol. Quantitative real time PCR analysis was performed in duplicates with TaqMan Gene Expression Assays according to the manufacturer's protocol (Applied Biosystems; 7500 Fast Real-time PCR System). 2.5 μl of the cDNA was amplified using probes for human fibrillin-1 (Hs00171191_m1), fibronectin (Hs01549940_m1), and ribosomal 18S RNA (HS99999901_s1) as internal control. Relative quantification was calculated by setting the signals from the non-treated sample divided by the signal for the 18S RNA to 1 (Applied Biosystems; 7500 System software version 1.3.0).

Semiquantitative Measurement of Extracellular Matrix Deposition—The amount of extracellular matrix secreted by fibroblasts was determined in a microplate-based assay as published with some modifications (45). HSFs were seeded in 96-well plates (Costar, Corning Inc.) at a density of 1.7×10^4 cells/well in 50 μl of DMEM in quadruplicates. After 24 h, the

medium was changed to DMEM including different concentrations of homocysteine and cysteine and for the following 3 days, the medium was changed every 12 h. For a background control, four wells with 1.7×10^4 cells/well in 50 μl of DMEM were seeded 12 h before the end of the incubation period. This short culture period is not sufficient to produce a fibrillin-1 network and therefore, the cellular background can be assessed. The cells with the extracellular matrix layer were washed with PBS (general washing buffer) and fixed in 50 μl of ice-cold 70% methanol, 30% acetone. Cells were washed again, blocked for 60 min with 75 μl of PBS-G, and incubated with 50 μl of the primary monoclonal fibrillin-1 F2 (1:1000) (10) or FN-15 (1:1000) antibody diluted in PBS-G for 2 h. After washing, the cells were incubated for 2 h with 50 μl of goat anti-rabbit (1:100) or goat anti-mouse horseradish peroxidase conjugate (1:200) diluted in PBS-G. After washing with PBS the color reaction was performed as described under "Solid Phase Binding Assays" and the absorption at 492 nm was measured.

Analysis of Coacervation—The coacervation experiments were carried out as described in detail elsewhere (46). For our studies, we used polypeptides EP20-24-24/36 including the two cysteines in the sequence encoded by exon 36 and EP20-24-24 without the exon 36-encoded protein sequence as a control (27). 25 μM polypeptide in 50 mM Tris (pH 7.2), 1.5 M NaCl was incubated without (control), with 300 μM homocysteine, or with 300 μM cysteine for 1 h on ice prior to the coacervation experiment. Coacervation was measured at 440 nm in a Shimadzu UV-2401PC UV-visible recording spectrophotometer with a temperature and stir rate controller (Mandel Scientific). The initial temperature was set 5 °C below the coacervation temperature (T_c) and raised by 1 °C/min to a final target temperature 3–4 °C above T_c. The final temperature was kept constant for 40 min to record the maturation phase. The temperature ramps were 24–35 °C for EP20-24-24 and 25–37 °C for EP20-24-24/36. T_c was noted as the onset of the increase in absorption and the results of the experiments are expressed as a shift of the coacervation temperature as compared with the control (ΔT_c). The curves were fitted using the MathWork software (Natick, MA) with the equation: $A = -a \times e^{(-k_c \times t)} + b \times e^{(-k_m \times t)} + c$, where A is the absorption at 440 nm, a, b, and c are proportionality factors, k_c is the rate constant for the coacervation, and k_m is the rate constant for the maturation. The velocities for the coacervation and maturation were calculated as $V_c = a \times k_c$ and $V_m = b \times k_m$. Details of this method are explained in Ref. 46.

RESULTS

Homocysteinylation of Fibrillin-1 Fragments—The protein fragments used in this study are well characterized N- and C-terminal halves (rFBN1-N and rFBN1-C, respectively), spanning the entire fibrillin-1 molecule (Fig. 1*A*). Because the interaction repertoire of these molecules was studied extensively, they serve as valuable tools to elucidate mechanistic aspects of fibrillin-1/microfibril assembly. The fragments were incubated with 300 μM homocysteine or cysteine for 24 h. This is in the pathophysiological range of concentrations detected in the plasma of patients with severe forms of homocystinuria caused by CBS deficiency. In addition, this mimics the continuous

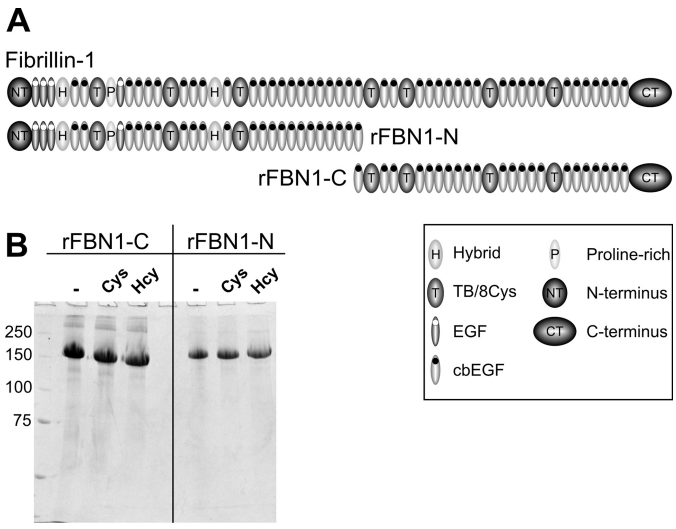

FIGURE 1. **Fibrillin-1 fragments used in this study.** *A*, schematic overview of the two recombinant halves of fibrillin-1, rFBN1-N (N terminus) and rFBN1-C (C terminus). *TB/8Cys*, transforming growth factor-β binding protein-like module/8 cysteine motif. *B*, the fragments were either not treated (−) or treated with 300 μM homocysteine (*Hcy*) or cysteine (*Cys*), and aliquots of 10 μg were then separated by 7.5% SDS-PAGE under reducing conditions (20 mM DTT). There are no major differences detectable between the modified and non-modified fragments, notably no degradation. Positions of molecular marker proteins are indicated in kilodaltons.

exposure of extracellular proteins to lower concentrations of homocysteine, found in patients with various forms of homocysteinemia (3). Fig. 1*B* shows that there is no degradation observed for rFBN1-N and rFBN1-C after modification with cysteine or homocysteine as judged by SDS-PAGE analysis under reducing conditions. Occasionally, rFBN1-N but not rFBN1-C tended to precipitate after homocysteinylation.

Fibrillin-1 N- to C-terminal Self-interaction—We used a well established solid phase binding assay to address the question, if the N- to C-terminal self-interaction of fibrillin-1 is affected by homocysteinylation. This self-interaction is considered one of the early steps in the biogenesis of microfibrils. In this assay, the N-terminal half (rFBN1-N) was coated and the C-terminal half (rFBN1-C) was added as soluble ligand in serial dilutions. Fig. 2 shows that homocysteinylation of rFBN1-N (Fig. 2*A*) and rFBN1-C (Fig. 2*B*) lowers the apparent affinity and the overall binding capacity to the respective counterpart. It clearly demonstrates that homocysteinylation is interfering with the capability of the N and C terminus to interact with each other. This effect is specific for homocysteine, because modification with cysteine does not result in a significant change in the N- to C-terminal binding of rFBN1-C to rFBN1-N. The homocysteinylation of the N terminus tends to more strongly affect the overall binding (reduction to 72.9% of the control) than the apparent affinity to the C terminus (~1.2-fold higher K_D) (Fig. 2*C*). However, the difference did not reach statistical significance. In contrast, the modification of rFBN1-C with homocysteine led to a dramatically increased apparent K_D indicating a lower affinity for the N-terminal half of fibrillin-1 (~12-fold lower) and reduces the overall binding to 81.9% of the control (Fig. 2*D*). The strong increase in the apparent K_D of the binding of the homocysteinylated C terminus to the N terminus ($p = 0.046$, Fig. 2*D*) and the reduction in binding of the homocys-

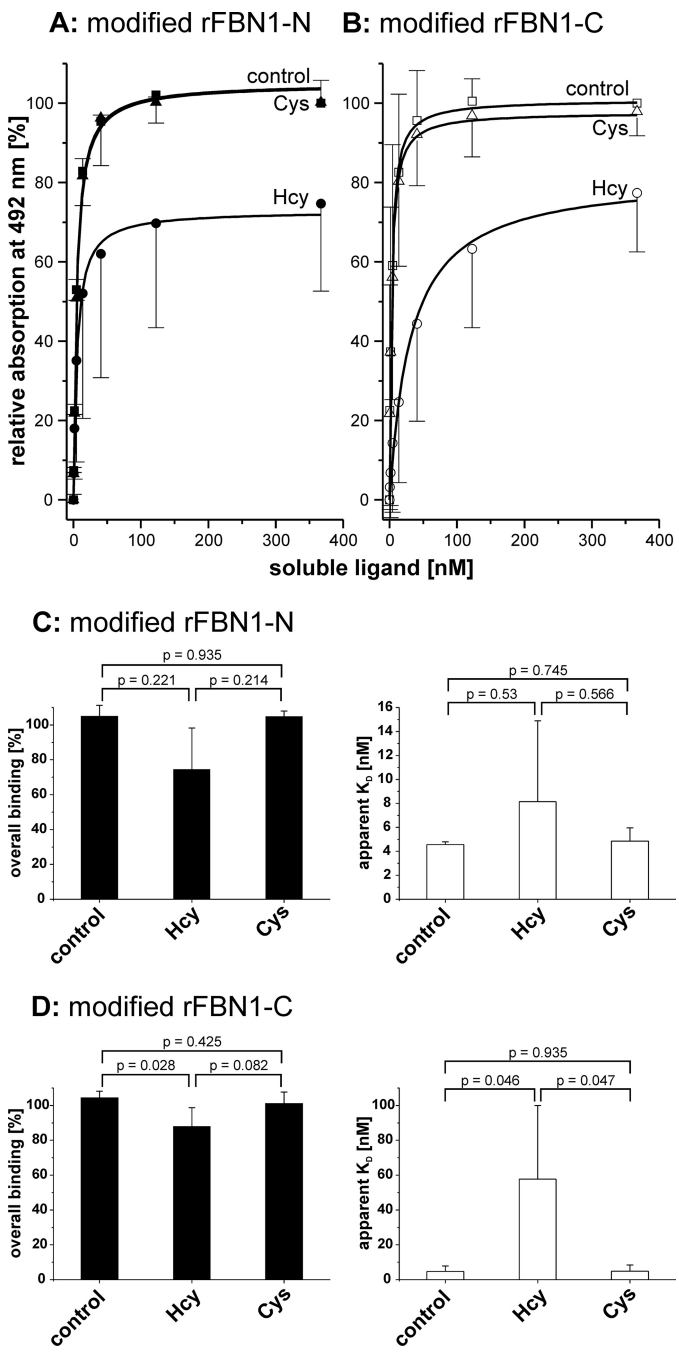

FIGURE 2. **Fibrillin-1 N- to C-terminal self-interaction is impaired by homocysteinylation.** Solid phase binding assays with immobilized rFBN1-N and soluble rFBN1-C were used to assess the effect of homocysteinylation on the N- to C-terminal self-interaction process. *A*, consequences on the interaction between modified rFBN1-N with non-modified rFBN1-C using homocysteinylated (300 μM Hcy, ●), cysteinylated (300 μM Cys, ▲), or non-treated (control, ■) rFBN1-N ($n = 2$). *B*, consequences on the binding of modified rFBN1-C to non-modified rFBN1-N, using homocysteinylated (300 μM Hcy, ○), cysteinylated (300 μM Cys, △), or non-treated (control, □) rFBN1-C ($n = 4$). Notice that there remains always one binding partner unmodified in both panels. In *A* and *B*, data are shown as percentage of the highest soluble ligand concentration of the non-treated control and represent mean ± S.D. The signal at 492 nm for the controls was in all experiments >1.0 absorption units. *C* and *D*, statistical analysis of data shown in *A* and *B* for the overall binding and the apparent K_D of N- to C-terminal self-interactions with modified rFBN1-N (*C*) or rFBN1-C (*D*). The *bars* represent mean ± S.D. of the overall binding (%) derived from the horizontal asymptote of the hyperbolic fit of individual experiments and the apparent K_D (nM) representing the ligand concentration at 50% overall binding. The statistical significance was calculated using the two-sided Student's *t* test. *p* values <0.05 are considered statistically significant.

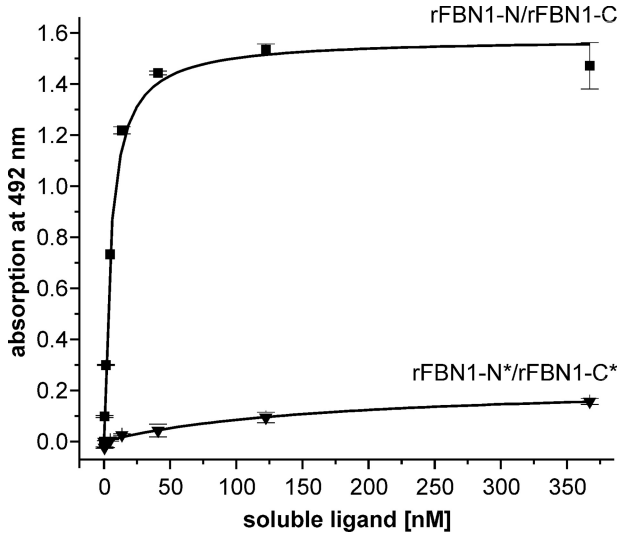

FIGURE 3. **Homocysteinylation of N- and C-terminal fibrillin-1 fragments results in a complete loss of self-interaction.** N and C termini of fibrillin-1 were homocysteinylated (300 μM) and tested in a solid phase binding assay using immobilized rFBN1-N and soluble rFBN1-C. The control showed the expected hyperbolic binding curve (rFBN1-N/rFBN1-C, ■). Modification of both binding ligands with homocysteine (*) resulted in an almost complete loss of the ability to self-interact (rFBN1-N*/rFBN1-C*, ▼). Representative data are shown as mean ± S.D. values of duplicates.

teinylated C terminus to the N terminus ($p = 0.028$, Fig. 2*D*) are statistically significant. To simulate the effect of homocysteine on full-length fibrillin-1, we performed a solid phase binding assay using simultaneously both, homocysteinylated N and C termini (Fig. 3). Modification of both fibrillin-1 termini resulted in an almost complete reduction of the self-interaction as compared with the homocysteinylation of only one ligand (compare Figs. 2, *A* and *B*, with 3). These data indicate that both self-interaction sites, on the N and C terminus, are functionally affected by homocysteinylation.

Multimerization of the C Terminus Is Reduced by Homocysteinylation—Recently, we showed that disulfide bond-mediated multimerization of the C terminus of fibrillin-1 is a necessary prerequisite for the N- to C-terminal self-interaction (13). To test if multimerization of the C terminus is affected by homocysteine, we separated multimers from monomers using gel filtration. After incubation with homocysteine or cysteine, the multimers were subjected to SDS-PAGE under non-reducing conditions and silver-stained (Fig. 4, *A–C*). The amount of multimers was reduced at homocysteine concentrations of 300 μM and higher. Full reduction is achieved using 20 mM DTT, which served as a control (Fig. 4*A*, DTT). The monomers resulting from homocysteinylation appear to migrate at a lower apparent molecular weight correlating with the homocysteine concentration in the sample (Fig. 4*A*, *arrowheads*). The consequence of homocysteine on the multimerization of the fibrillin-1 C terminus is significantly more specific for homocysteine because cysteine in the same concentration range only had a little effect (Fig. 4*B*). Only a very faint protein band of the monomeric size appears at a cysteine concentration of 1 mM (Fig. 4*B*, *arrowheads*). This band migrated slightly faster then the fragment reduced with DTT, but not as fast as the homocysteine-modified fragment (Fig. 4*C*). Analyzing the same set of samples after modification with 1 mM homocysteine, cysteine, or DTT sub-

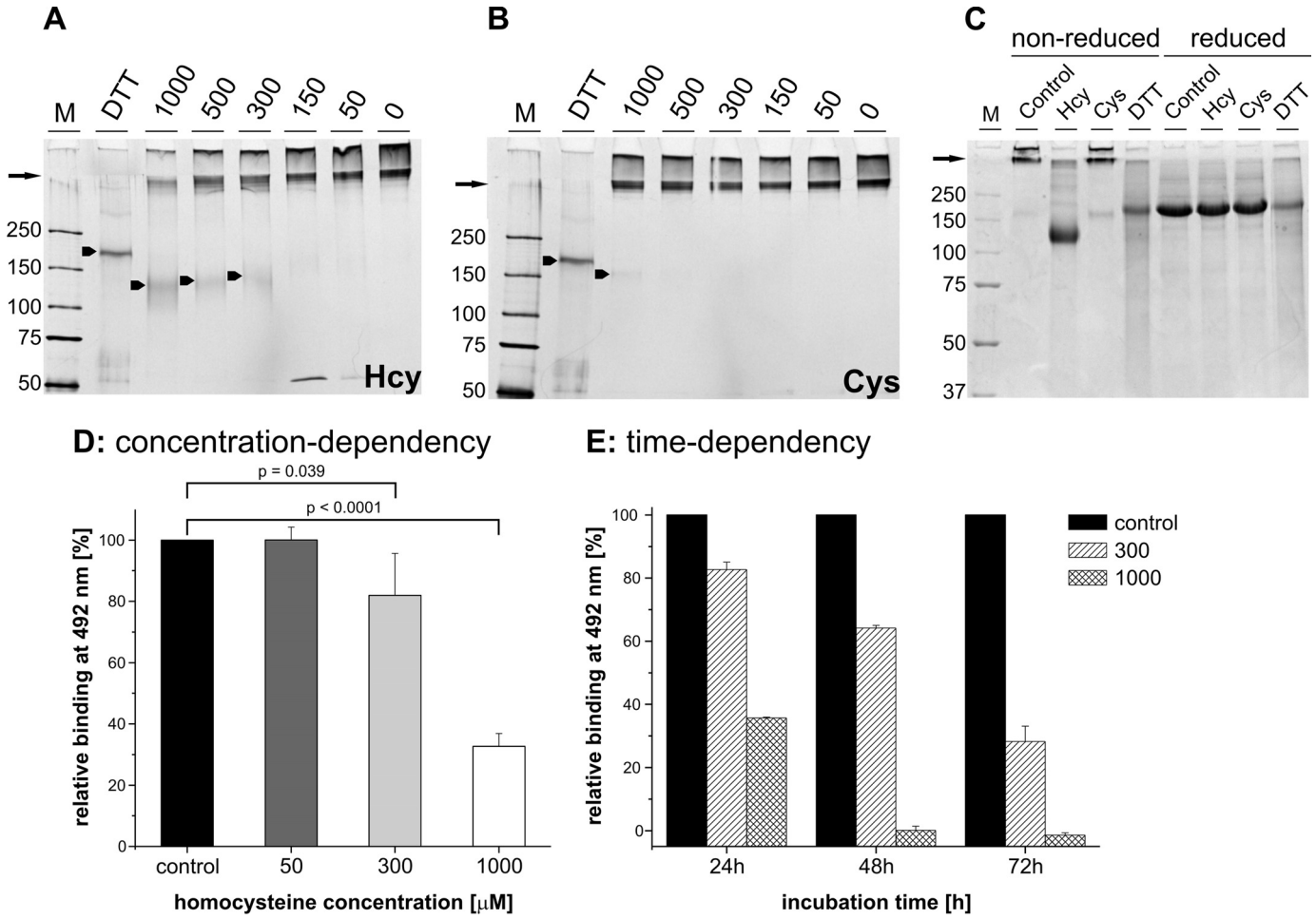

FIGURE 4. **Homocysteine reduces the amount of fibrillin-1 C-terminal multimers and dose and time dependently affects the fibrillin-1 self-interaction.** Multimers of rFBN1-C were purified using gel filtration and incubated with different concentrations of homocysteine (*A*, Hcy) and cysteine (*B*, Cys), as indicated in micromolar. Shown are silver-stained gels after non-reducing SDS-PAGE (4–20%). Incubation with 1 mM DTT served as controls. Monomers of rFBN1-C are indicated by *arrowheads*. *Arrows* indicate the border between stacking and separating gels. *C*, multimers of rFBN1-C were first incubated with 1 mM homocysteine (*Hcy*), cysteine (*Cys*), or DTT compared with a non-treated control and then separated by 4–20% gradient SDS-PAGE under either non-reduced or reduced (additional 20 mM DTT) conditions as indicated. Note the qualitative difference between the homocysteinylated proteins analyzed under reduced *versus* non-reduced conditions. Positions of molecular marker proteins (*M*) are indicated in kilodaltons. *D*, solid phase binding assay of soluble rFBN1-C (734 nM) homocysteinylated with 50–1000 μM as indicated and coated non-modified rFBN1-N. The *bars* represent the relative binding compared with the control with non-modified rFBN1-C (100% binding). Statistically significant differences compared with the control are indicated ($p \leq 0.05$ level). *E*, rFBN-1C was homocysteinylated with 300 and 1000 μM homocysteine for 24, 48, and 72 h as indicated, and the N- to C-terminal fibrillin-1 self-interaction was analyzed as in *D* with 734 nM soluble rFBN1-C. The relative absorption for each time point is blotted compared with non-treated controls (100% binding). Data are shown as mean ± S.D. values of duplicates.

sequently under reducing conditions (20 mM DTT) resulted in bands migrating at identical molecular weight positions (Fig. 4*C*). This result indicates that the apparent lower molecular weight is caused by reversible modifications of the proteins. In the self-interaction assay, the reduction in binding of the homocysteinylated C terminus of fibrillin-1 to the N terminus is dose-dependent with respect to the homocysteine concentration used for modification (Fig. 4*D*). This correlates with the dose dependence observed for the homocysteine-induced reduction of the C-terminal multimers. To analyze the time course of fibrillin-1 homocysteinylation, we incubated the rFBN1-C fragment with different concentrations of homocysteine for various time points and tested self-interaction with non-modified rFBN1-N (Fig. 4*E*). The 72-h incubation with 300 μM homocysteine resulted in a similar reduction of the self-interaction than the 24-h incubation with 1000 μM. Therefore, it is possible to use short term exposure of fibrillin-1 fragments with high homocysteine concentrations (up to 1000 μM) to simulate the long term exposure to lower homocysteine concentrations, as it occurs in patients.

Binding of Homocysteinylated Fibrillin Fragments to Heparin—Fibrillin-1 interacts with heparin and heparan sulfate through several domains distributed throughout the molecule, including the N and C terminus (43, 47, 48). Therefore, we tested if homocysteinylation interferes with binding of fibrillin-1 fragments to heparin (Fig. 5). Homocysteinylation of rFBN1-N and rFBN1-C resulted in a significant decrease in binding to heparin. The modification with cysteine also reduced the binding capability to a similar extent and the differences between the two types of modifications were not statistically significant. The observation of nonspecific consequences of homocysteinylation compared with cysteinylation strengthens the relevance of the homocysteine-specific effects observed for the fibrillin-1 N- to C-terminal self-interaction described above.

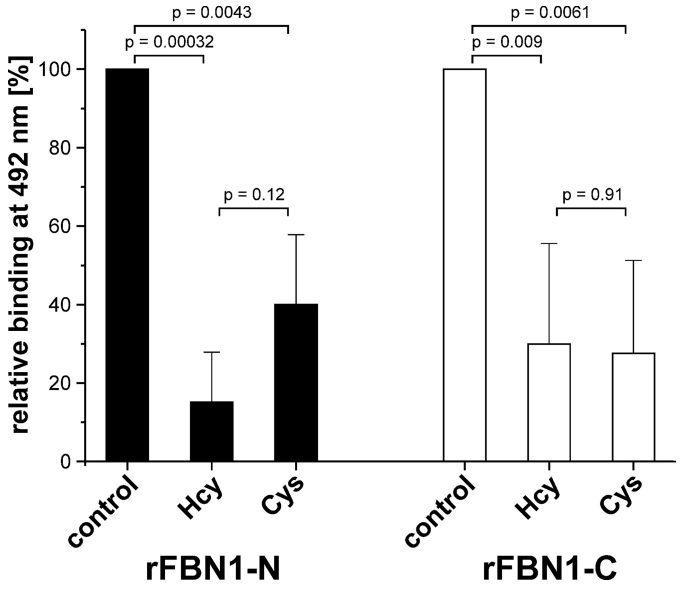

FIGURE 5. **Homocysteinylation and cysteinylation affect binding of the fibrillin-1 N and C terminus to heparin.** Solid phase binding assays were used to assess the effect of homocysteinylation of rFBN1-N and rFBN1-C on the interaction with BSA-heparin. Soluble rFBN1-N and rFBN1-C (both 734 nM) were used as soluble ligands and BSA-heparin as immobilized ligand. Homocysteinylation (300 μM) and cysteinylation (300 μM) reduced the binding to BSA-heparin compared with non-modified rFBN1-N and non-modified rFBN1-C (controls, 100%). Representative data are shown as mean ± S.D. values of three experiments. The original signal at 492 nm for the controls was in all experiments between 0.4 and 1.0 absorption units. The significance was calculated using the two-sided Student's *t* test.

Deposition of Fibrillin-1 by HSFs Is Reduced in the Presence of Homocysteine—To assess the effect of homocysteine on the deposition of fibrillin-1 into the extracellular matrix, HSFs were grown in the presence of 1000 μM homocysteine or cysteine for 4 days and analyzed by immunofluorescence. The relatively high homocysteine concentration was required because the concentration of free (active) homocysteine/cysteine is reduced in the presence of serum components such as BSA (49). The matrix deposition of fibrillin-1 was always significantly reduced after treatment with homocysteine, but not with cysteine, whereas the deposition of fibronectin was not affected (Fig. 6*A*). A semi-quantitative analysis of the fibrillin-1 and fibronectin network formation after treatment with homocysteine showed a significant and dose-dependent reduction for the fibrillin-1 network, but not for the fibronectin network (Fig. 6*B*). No significant reduction could be detected with this assay for the fibrillin-1 matrix deposited by HSFs in the presence of cysteine. To additionally test whether other metabolites altered in homocystinuria patients influence the fibrillin-1 network formation, HSFs were treated with reduced cysteine (50 *versus* 300 μM for the control) and high methionine (1 mM *versus* 30–40 μM for the control) (50). No changes in the fibrillin-1 network formation were detected under these conditions (data not shown).

Examination of mRNA levels by quantitative real time PCR showed a slight decrease of fibrillin-1 (16.8%) and fibronectin (8.3%) expression after homocysteine treatment, and a stronger reduction in fibrillin-1 (35.4%) and fibronectin (31.1%) expression after incubation with cysteine (Fig. 6*C*). These slightly reduced mRNA levels do not explain the specificity of homocysteine in reducing fibrillin-1 deposition by cells. Analysis of secreted fibrillin-1 and fibronectin in the cell culture medium by dot-blotting showed no differences between controls and homocysteine or cysteine-treated samples (Fig. 6*D*). We conclude that reduced formation of the fibrillin-1 network after incubation with homocysteine represents a deposition defect rather than deficient transcription or secretion.

Coacervation Properties of Elastin-like Polypeptides Are Altered upon Homocysteinylation—To assess the effect of homocysteine on elastin-like polypeptides, we used EP20-24-24 and EP20-24-24/36 containing the protein sequence encoded by exon 36 with the sole two cysteines found in human tropoelastin (Fig. 7*A*). The cysteines are engaged in an intramolecular disulfide bond (24). After homocysteinylation only, we observed a statistically significant increase in the coacervation temperature of 1.4 °C as compared with the control ($p = 0.003$, Fig. 7*B*). This was not observed after incubation with cysteine, ruling out an effect of the sole presence of a thiol group containing reagent and demonstrating the specificity for homocysteine. The coacervation temperature of the control polypeptide EP20-24-24 did not change significantly after incubation with either homocysteine or cysteine. Interestingly, the velocity for the coacervation and the maturation stage does not change in the presence of homocysteine (Fig. 7*C*). This is different as compared with other factors affecting the coacervation temperature, such as salt and other proteins of the elastic fiber system, which also affect either the velocity of coacervation or maturation, or both (27, 46).

DISCUSSION

The genetic disorder homocystinuria caused by CBS deficiency and Marfan syndrome overlap in some clinical symptoms, primarily in the skeletal system and the eye. This led originally to the hypothesis that fibrillin-1 is a target for homocysteine, which has been confirmed by us and others (35, 36). For the work presented here, we asked the question, does homocysteinylation affect the function of components of the microfibril/elastic fiber system, including fibrillin-1 and tropoelastin. To assess effects of homocysteinylation on fibrillin-1 self-interaction, correctly folded and well characterized N- and C-terminal halves of fibrillin-1 were utilized (38, 52). Studies with full-length fibrillin are currently hampered by its propensity to aggregate (15). A second aspect of this project focused on the consequences of homocysteinylation on the disulfide bond in tropoelastin as assessed by an elastin-like polypeptide, which includes the two disulfide bond-forming cysteines located in domain 36 of human tropoelastin (24).

We demonstrate here that homocysteinylation reduced significantly N- to C-terminal fibrillin-1 self-interaction properties, which represent a critical step in the biogenesis of microfibrils. Furthermore, homocysteinylation affected the multimerization of the fibrillin-1 C terminus. Both effects were specific for homocysteine as compared with cysteine. Recently, we demonstrated that the affinity of the fibrillin-1 N- to C-terminal self-interaction is strictly dependent on the multimerization state of the C terminus, ranging from very low affinity for monomers to intermediate affinities for oligomers with 3–7 subunits and to very high affinity for multimers with 8–12 sub-

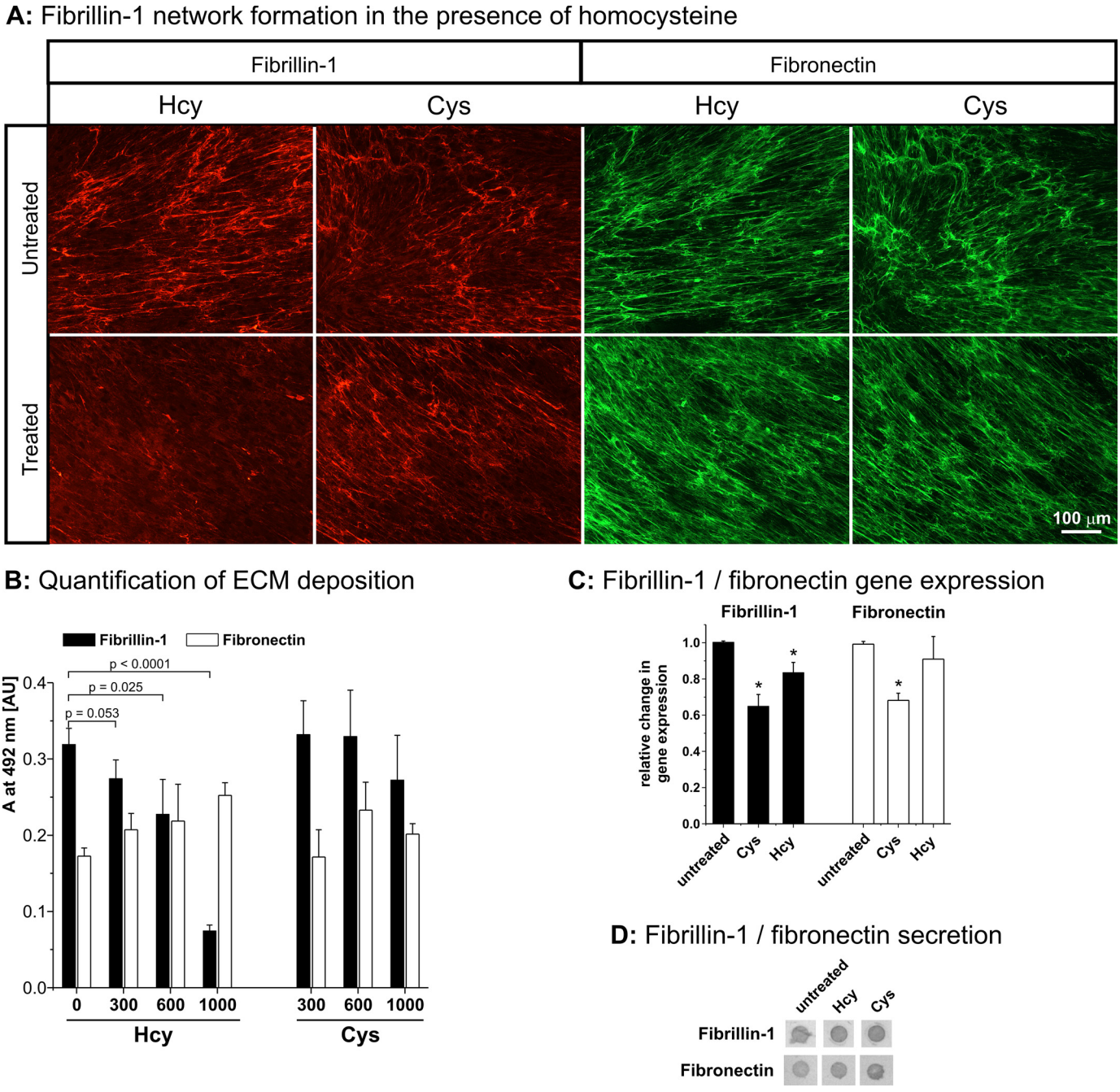

FIGURE 6. **Functional consequence of homocysteine and cysteine on the fibrillin-1 network formation in cell culture.** HSFs were used to study the effect of homocysteine and cysteine on the formation of the extracellular fibrillin-1 network. *A*, immunofluorescence of fibrillin-1 (*red*) and fibronectin (*green*) after incubation with 1000 μM homocysteine (*Hcy*) or cysteine (*Cys*) for 4 days. Note that the fibrillin-1 network is greatly reduced only in the presence of homocysteine. The experiments were repeated with cells from two different donors with identical results. The *scale bar* represents 100 μm. *B*, quantification of fibrillin-1 (*black bars*) and fibronectin (*white bars*) deposition by a microplate-based assay (see "Experimental Procedures"). *Bars* represent mean ± S.D. values of 4 data points. The statistical significance was calculated with a two-sided Student's *t* test and the *p* values are indicated. *C*, to control for gene expression, quantitative real time PCR with TaqMan probes for human FBN1 and FN was performed after growing the fibroblasts for 4 days in the presence of 1000 μM homocysteine or cysteine. Ribosomal 18S RNA was used as an internal standard. The *asterisk* indicates a statistically significant difference compared with the respective control. *D*, the cell culture medium (25 μl) from the final 12-h incubation period of the experiment shown in *A* was analyzed by dot-blotting using specific antibodies against fibrillin-1 and fibronectin as indicated. Notice that the amount of secreted soluble fibrillin-1 or fibronectin is similar in all samples.

units (13). In that study, multimerization was shown to be mediated by solvent-exposed intermolecular disulfide bonds. In light of this, we conclude from our data presented here that homocysteine interferes with intermolecular disulfide bonds stabilizing the high molecular weight assemblies mediated through the C terminus, and leading to the loss of apparent affinity to the N terminus. This modification requires the higher nucleophilic reactivity of homocysteine compared with cysteine, because cysteine in identical concentrations was non-reactive. It is likely that homocysteine reduces accessible cysteine-cysteine bonds and forms mixed cysteine-homocysteine disulfides. This notion is further supported by the fact that homocysteine-modified rFBN1-C monomers, which migrate slightly faster in polyacrylamide gel electrophoresis than the

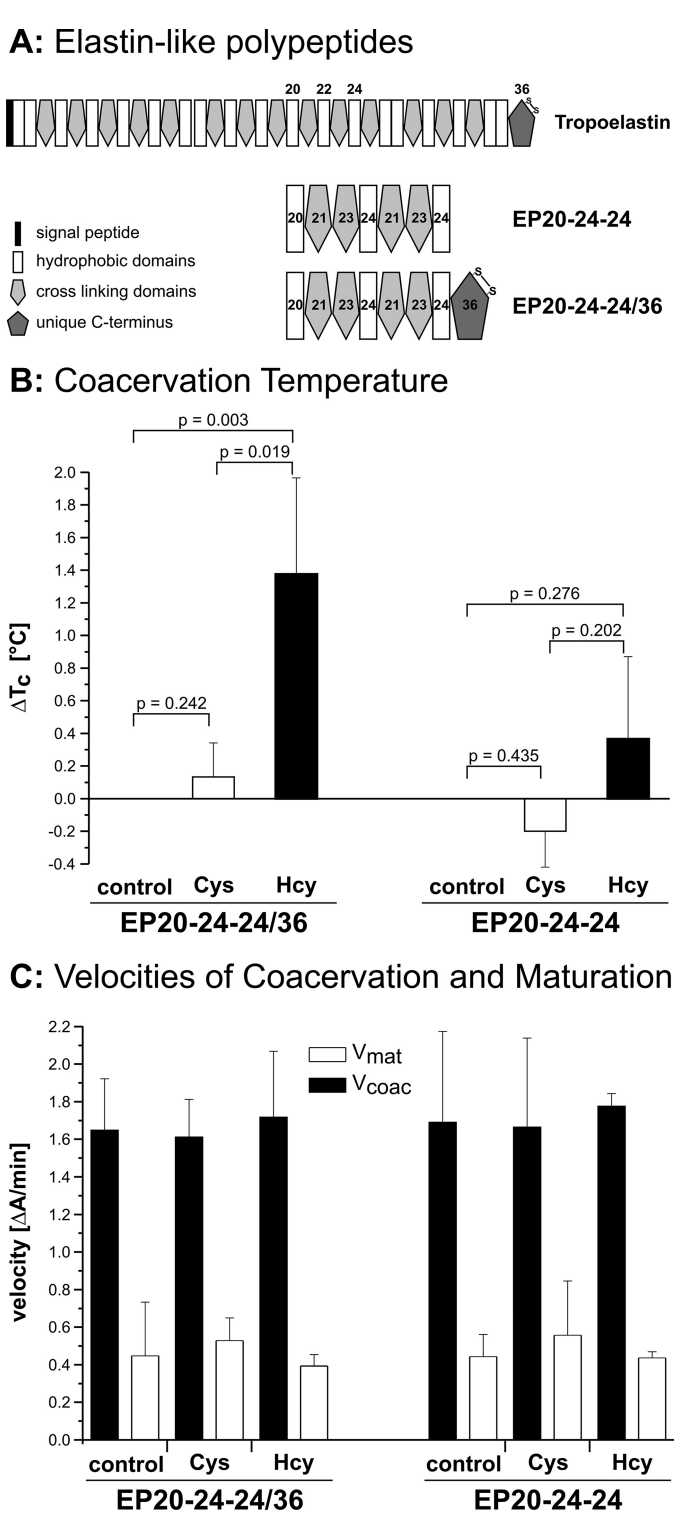

FIGURE 7. **Effect of homocysteine on the coacervation and maturation of elastin-like polypeptides.** Coacervation was used to study the effect of homocysteine on elastin-like polypeptides. *A*, schematic overview of the domain structure of human tropoelastin and the two elastin-like polypeptides EP20-24-24 and EP20-24-24/36. Relevant domain numbers are indicated. *B*, analysis of the coacervation temperature after incubation of the polypeptides with 300 μM homocysteine (*Hcy*) or 300 μM cysteine (*Cys*). The coacervation temperatures are indicated as ΔT_c compared with the coacervation temperature of non-modified elastin-like peptides. T_c for EP20-24-24 = 28.7 °C (±0.3 °C) and EP20-24-24/36 = 28.6 °C (±0.8 °C). Note that only modification with homocysteine significantly increased the coacervation temperature (+1.4 °C) of EP20-24-24/36, but not modification with cysteine (+0.1 °C). Indicated *p* values were calculated using a two-sided Student's *t* test. *C*, analysis of the velocities of coacervation (V_{coac}, *black bars*) and maturation (V_{mat}, *white bars*) after modification with homocysteine (*Hcy*) and cysteine (*Cys*) are indicated in ΔA at 440 nm/min. The experiments were repeated 3–5 times with different batches of polypeptides. The mean ± S.D. are indicated.

non-homocysteinylated monomers, adopt a normal migration pattern after additional reduction with dithiothreitol. In addition to the above discussed mechanism, the following factors might also mechanistically contribute to the loss of N- to C-terminal self-interaction properties. Homocysteinylation of fibrillin-1 led to subtle structural changes in cbEGF domains (35). In this regard, structural modifications in cbEGF41-43, which has been shown to contain the binding domain for the N terminus, may be a critical factor (13). We and others have previously shown that the N- to C-terminal fibrillin-1 self-interaction is calcium dependent (14, 15), and that homocysteinylation abolishes calcium binding to cbEGF domains in fibrillin-1 (35). With this background, homocysteinylation of the N- or C-terminal half might affect their calcium-binding properties required for self-assembly. In addition, it is possible that homocysteine modifies the non-paired cysteine residue in the first hybrid domain of the fibrillin-1 N terminus necessary for the self-assembly process (53). Given the additive effect when both, the fibrillin-1 N and C terminus, are homocysteinylated, we suggest that a combination of the above described mechanisms is likely to lead to the observed functional consequences.

In cell culture the deposition of fibrillin-1 is reduced in the presence of homocysteine, but not in the presence of cysteine. This clearly demonstrates that the observed reduction in fibrillin-1 N- to C-terminal self-interaction upon homocysteinylation translates into a reduced network formation in cell culture. It was previously shown using smooth muscle cells that 300 μM homocysteine did not reduce the deposition of fibrillin-1 (33). We observed with fibroblasts a marked reduction of the fibrillin-1 network formation with 1000 μM homocysteine, but not with 300 μM. This suggests a threshold effect that could be attributed to the serum present in the culture medium required for a proper fibrillin-1 deposition. Albumin is a target for homocysteine and its abundance in serum could reduce the effective homocysteine concentration (49, 57). In addition, a threshold effect for homocysteine has been recently described in a Cbs-deficient mouse model (59).

Giusti *et al.* (54) recently demonstrated a positive correlation of the severity of cardiovascular manifestations, including aortic involvement, with mildly elevated homocysteine levels in individuals with Marfan syndrome. Aortic aneurysms are a common symptom in Marfan syndrome and can lead to death. In light of this, it is possible that mutations in fibrillin-1 further contribute to its susceptibility for homocysteinylation potentially enhancing the above discussed molecular consequences on fibrillin-1 self-assembly and thus further contributing to the pathogenetic sequence.

Fibrillin-1 has been shown to interact with heparin/heparan sulfate in various regions of fibrillin-1 (43, 47, 48). Here, we show that homocysteinylation of fibrillin-1 reduces heparin binding to fibrillin-1, similar to cysteinylation. In this case, the reactive nucleophilic potential of the cysteine sulfhydryl group

is sufficient to modify intra- or inter-molecular disulfide bonds in heparin/heparan sulfate-binding regions of fibrillin-1. These results exemplify that the different disulfide bonds in fibrillin-1 vary in their susceptibility for reduction by thiol-containing compounds. A molecular targeting hypothesis was recently developed stating that homocysteine attacks not all but only specific disulfide bonds or free cysteines in proteins (55, 56). To render free cysteines as targets for homocysteinylation, they have to be solvent exposed and must have a relatively low pK_a value ($<$8.15), as defined by the sequence context of a given protein. Disulfide bonds have to be solvent accessible and contain high energy as estimated from the relative angles of the two individual cysteines forming the disulfide bond, expressed as the dihedral strain energy ($>$17.8 kJ/mol). In that study, cbEGF modules 32–34 of fibrillin-1 were a predicted target for homocysteinylation, which correlates with experimental data (36). Given the large number of disulfide bonds in fibrillin-1, this prediction algorithm may prove useful in combination with our experimental data to identify potential cysteine target residues for homocysteinylation and design new and testable hypotheses for the pathogenetic mechanisms involved in Marfan syndrome and homocystinuria.

Animal models of homocystinuria, including mouse, chick, and mini-pig, show a phenotype in the elastic fiber system of lung and aorta. Methionine-induced hyperhomocysteinemia in chick lungs for example, led to thin and clearly disrupted elastic fibers in the parabronchi and air capillaries (60). Moreover, it was shown that the desmosin content, a marker for correctly cross-linked elastin, is markedly reduced. In addition, the authors showed that alveolar lung development in mice is impaired at early stages leading to enlarged airways and emphysema-like appearance. Additionally, a study using mini-pigs showed that mild hyperhomocysteinemia led to the deterioration of the elastin structure in the arterial media (58). Our experiments, using the elastin-like polypeptide EP20-24-24/36 as an experimental model for tropoelastin assembly showed that homocysteine increased the coacervation temperature of this polypeptide by 1.4 °C. This effect was specific for homocysteine as it was not observed after incubation with cysteine. It is likely, that homocysteine exerted this effect by modifying the disulfide bond in C-terminal domain 36, because it was not observed for the control polypeptide EP20-24-24 lacking domain 36. It should be noted that the velocities of coacervation and maturation did not change upon homocysteinylation. This is in contrast to elastic fiber proteins such as fibrillin-1, fibulin-5, or MAGP-1, which typically affected the velocity of maturation of elastin-like polypeptides without changing the coacervation temperature (46). An alteration of tropoelastin coacervation properties observed after homocysteinylation may indicate that homocysteine interferes with the biogenesis of elastic fibers, with potential pathogenetic consequences in the structure, stability, and functionality of elastic fibers. Such microscopic defects may accumulate over time because there is virtually no turnover of elastin observed (51).

In conclusion, we describe for the first time mechanistic consequences of fibrillin-1 homocysteinylation, which provides the basis for new and testable hypotheses to address its contribution in the pathogenetic sequence leading to some of the connective tissue phenotypes in CBS-deficient homocystinuria. Moreover, for the first time we provided *in vitro* evidence that tropoelastin is a target for homocysteinylation.

Acknowledgment—We thank Dr. Lynn Sakai (Shriners Hospital for Children, Portland, OR) for generously providing the F2 anti-fibrillin-1 monoclonal antibody. We are grateful to Dr. Jean-Martin Laberge (Montreal Children's Hospital) for providing foreskin samples.

REFERENCES

1. Skovby, F., and Kraus, J. P. (2002) in *Connective Tissue and Its Heritable Disorders* (Royce, P. M., and Steinmann, B., eds) pp. 627–650, Wiley-Liss, New York
2. Ueland, P. M., Refsum, H., and Brattstrom, L. (1992) in *Atherosclerotic Cardiovascular Disease, Hemostasis, and Endothelial Function* (Francis, R. B. J., ed) pp. 183–236, Marcel Dekker, New York
3. Refsum, H., Ueland, P. M., Nygård, O., and Vollset, S. E. (1998) *Annu. Rev. Med.* **49,** 31–62
4. Gellekink, H., den Heijer, M., Heil, S. G., and Blom, H. J. (2005) *Semin. Vasc. Med.* **5,** 98–109
5. Hubmacher, D., Tiedemann, K., and Reinhardt, D. P. (2006) *Curr. Top. Dev. Biol.* **75,** 93–123
6. Kielty, C. M., Sherratt, M. J., Marson, A., and Baldock, C. (2005) *Adv. Protein Chem.* **70,** 405–436
7. Collod-Béroud, G., Le Bourdelles, S., Ades, L., Ala-Kokko, L., Booms, P., Boxer, M., Child, A., Comeglio, P., De Paepe, A., Hyland, J. C., Holman, K., Kaitila, I., Loeys, B., Matyas, G., Nuytinck, L., Peltonen, L., Rantamaki, T., Robinson, P., Steinmann, B., Junien, C., Béroud, C., and Boileau, C. (2003) *Hum. Mutat.* **22,** 199–208
8. Vollbrandt, T., Tiedemann, K., El-Hallous, E., Lin, G., Brinckmann, J., John, H., Bätge, B., Notbohm, H., and Reinhardt, D. P. (2004) *J. Biol. Chem.* **279,** 32924–32931
9. Suk, J. Y., Jensen, S., McGettrick, A., Willis, A. C., Whiteman, P., Redfield, C., and Handford, P. A. (2004) *J. Biol. Chem.* **279,** 51258–51265
10. Sakai, L. Y., Keene, D. R., and Engvall, E. (1986) *J. Cell Biol.* **103,** 2499–2509
11. Zhang, H., Apfelroth, S. D., Hu, W., Davis, E. C., Sanguineti, C., Bonadio, J., Mecham, R. P., and Ramirez, F. (1994) *J. Cell Biol.* **124,** 855–863
12. Corson, G. M., Charbonneau, N. L., Keene, D. R., and Sakai, L. Y. (2004) *Genomics* **83,** 461–472
13. Hubmacher, D., El-Hallous, E. I., Nelea, V., Kaartinen, M. T., Lee, E. R., and Reinhardt, D. P. (2008) *Proc. Natl. Acad. Sci. U.S.A.* **105,** 6548–6553
14. Marson, A., Rock, M. J., Cain, S. A., Freeman, L. J., Morgan, A., Mellody, K., Shuttleworth, C. A., Baldock, C., and Kielty, C. M. (2005) *J. Biol. Chem.* **280,** 5013–5021
15. Lin, G., Tiedemann, K., Vollbrandt, T., Peters, H., Batge, B., Brinckmann, J., and Reinhardt, D. P. (2002) *J. Biol. Chem.* **277,** 50795–50804
16. Mecham, R. P., and Davis, E. (1994) in *Extracellular Matrix Assembly and Structure* (Yurchenco, P. D., Birk, D. E., and Mecham, R. P., eds) pp. 281–314, Academic Press, New York
17. Carta, L., Pereira, L., Arteaga-Solis, E., Lee-Arteaga, S. Y., Lenart, B., Starcher, B., Merkel, C. A., Sukoyan, M., Kerkis, A., Hazeki, N., Keene, D. R., Sakai, L. Y., and Ramirez, F. (2006) *J. Biol. Chem.* **281,** 8016–8023
18. Wagenseil, J. E., and Mecham, R. P. (2007) *Birth Defects Res. Part C. Embryo Today* **81,** 229–240
19. Ramirez, F., and Rifkin, D. B. (2009) *Curr. Opin. Cell Biol.* **21,** 616–622
20. Isogai, Z., Ono, R. N., Ushiro, S., Keene, D. R., Chen, Y., Mazzieri, R., Charbonneau, N. L., Reinhardt, D. P., Rifkin, D. B., and Sakai, L. Y. (2003) *J. Biol. Chem.* **278,** 2750–2757
21. Sengle, G., Charbonneau, N. L., Ono, R. N., Sasaki, T., Alvarez, J., Keene, D. R., Bächinger, H. P., and Sakai, L. Y. (2008) *J. Biol. Chem.* **283,** 13874–13888
22. Ono, R. N., Sengle, G., Charbonneau, N. L., Carlberg, V., Bächinger, H. P., Sasaki, T., Lee-Arteaga, S., Zilberberg, L., Rifkin, D. B., Ramirez, F., Chu,

M. L., and Sakai, L. Y. (2009) *J. Biol. Chem.* **284,** 16872–16881
23. Mithieux, S. M., and Weiss, A. S. (2005) *Adv. Protein Chem.* **70,** 437–461
24. Brown, P. L., Mecham, L., Tisdale, C., and Mecham, R. P. (1992) *Biochem. Biophys. Res. Commun.* **186,** 549–555
25. Urry, D. W., and Long, M. M. (1977) *Adv. Exp. Med. Biol.* **79,** 685–714
26. Vrhovski, B., Jensen, S., and Weiss, A. S. (1997) *Eur. J. Biochem.* **250,** 92–98
27. Bellingham, C. M., Woodhouse, K. A., Robson, P., Rothstein, S. J., and Keeley, F. W. (2001) *Biochim. Biophys. Acta* **1550,** 6–19
28. Miao, M., Bellingham, C. M., Stahl, R. J., Sitarz, E. E., Lane, C. J., and Keeley, F. W. (2003) *J. Biol. Chem.* **278,** 48553–48562
29. Miao, M., Cirulis, J. T., Lee, S., and Keeley, F. W. (2005) *Biochemistry* **44,** 14367–14375
30. Clarke, A. W., Wise, S. G., Cain, S. A., Kielty, C. M., and Weiss, A. S. (2005) *Biochemistry* **44,** 10271–10281
31. Tu, Y., and Weiss, A. S. (2008) *Biomacromolecules* **9,** 1739–1744
32. Hill, C. H., Mecham, R., and Starcher, B. (2002) *J. Nutr.* **132,** 2143–2150
33. Majors, A. K., and Pyeritz, R. E. (2000) *Mol. Genet. Metab.* **70,** 252–260
34. Baumbach, G. L., Sigmund, C. D., Bottiglieri, T., and Lentz, S. R. (2002) *Circ. Res.* **91,** 931–937
35. Hubmacher, D., Tiedemann, K., Bartels, R., Brinckmann, J., Vollbrandt, T., Bätge, B., Notbohm, H., and Reinhardt, D. P. (2005) *J. Biol. Chem.* **280,** 34946–34955
36. Hutchinson, S., Aplin, R. T., Webb, H., Kettle, S., Timmermans, J., Boers, G. H., and Handford, P. A. (2005) *J. Mol. Biol.* **346,** 833–844
37. Reinhardt, D. P., Keene, D. R., Corson, G. M., Pöschl, E., Bächinger, H. P., Gambee, J. E., and Sakai, L. Y. (1996) *J. Mol. Biol.* **258,** 104–116
38. Jensen, S. A., Reinhardt, D. P., Gibson, M. A., and Weiss, A. S. (2001) *J. Biol. Chem.* **276,** 39661–39666
39. Uerre, J. A., and Miller, C. H. (1966) *Anal. Biochem.* **17,** 310–315
40. Ellman, G. L. (1959) *Arch. Biochem. Biophys.* **82,** 70–77
41. El-Hallous, E., Sasaki, T., Hubmacher, D., Getie, M., Tiedemann, K., Brinckmann, J., Bätge, B., Davis, E. C., and Reinhardt, D. P. (2007) *J. Biol. Chem.* **282,** 8935–8946
42. Tiedemann, K., Sasaki, T., Gustafsson, E., Göhring, W., Bätge, B., Notbohm, H., Timpl, R., Wedel, T., Schlötzer-Schrehardt, U., and Reinhardt, D. P. (2005) *J. Biol. Chem.* **280,** 11404–11412
43. Tiedemann, K., Bätge, B., Müller, P. K., and Reinhardt, D. P. (2001) *J. Biol. Chem.* **276,** 36035–36042
44. Tangemann, K., and Engel, J. (1995) *FEBS Lett.* **358,** 179–181
45. Wachi, H., Sato, F., Murata, H., Nakazawa, J., Starcher, B. C., and Seyama, Y. (2005) *Clin. Biochem.* **38,** 643–653
46. Cirulis, J. T., Bellingham, C. M., Davis, E. C., Hubmacher, D., Reinhardt, D. P., Mecham, R. P., and Keeley, F. W. (2008) *Biochemistry* **47,** 12601–12613
47. Cain, S. A., Baldock, C., Gallagher, J., Morgan, A., Bax, D. V., Weiss, A. S., Shuttleworth, C. A., and Kielty, C. M. (2005) *J. Biol. Chem.* **280,** 30526–30537
48. Cain, S. A., Baldwin, A. K., Mahalingam, Y., Raynal, B., Jowitt, T. A., Shuttleworth, C. A., Couchman, J. R., and Kielty, C. M. (2008) *J. Biol. Chem.* **283,** 27017–27027
49. Sengupta, S., Chen, H., Togawa, T., DiBello, P. M., Majors, A. K., Büdy, B., Ketterer, M. E., and Jacobsen, D. W. (2001) *J. Biol. Chem.* **276,** 30111–30117
50. Mudd, S. H., Levy, H. L., and Skovby, F. (1995) in *The Metabolic and Molecular Bases of Inherited Disease* (Scriver, C. R., Beaudet, A. L., Sly, W. S., and Valle, D., eds) pp. 1279–1327, McGraw-Hill Publishing Co., New York
51. Shapiro, S. D., Endicott, S. K., Province, M. A., Pierce, J. A., and Campbell, E. J. (1991) *J. Clin. Invest.* **87,** 1828–1834
52. Brinckmann, J., Hunzelmann, N., El-Hallous, E., Krieg, T., Sakai, L. Y., Krengel, S., and Reinhardt, D. P. (2005) *Arthritis Res. Ther.* **7,** R1221–R1226
53. Reinhardt, D. P., Gambee, J. E., Ono, R. N., Bächinger, H. P., and Sakai, L. Y. (2000) *J. Biol. Chem.* **275,** 2205–2210
54. Giusti, B., Porciani, M. C., Brunelli, T., Evangelisti, L., Fedi, S., Gensini, G. F., Abbate, R., Sani, G., Yacoub, M., and Pepe, G. (2003) *Eur. Heart J.* **24,** 2038–2045
55. Glushchenko, A. V., and Jacobsen, D. W. (2007) *Antioxid. Redox Signal.* **9,** 1883–1898
56. Sundaramoorthy, E., Maiti, S., Brahmachari, S. K., and Sengupta, S. (2008) *Proteins* **71,** 1475–1483
57. Sengupta, S., Wehbe, C., Majors, A. K., Ketterer, M. E., DiBello, P. M., and Jacobsen, D. W. (2001) *J. Biol. Chem.* **276,** 46896–46904
58. Charpiot, P., Bescond, A., Augier, T., Chareyre, C., Fraterno, M., Rolland, P. H., and Garçon, D. (1998) *Matrix Biol.* **17,** 559–574
59. Gupta, S., Kühnisch, J., Mustafa, A., Lhotak, S., Schlachterman, A., Slifker, M. J., Klein-Szanto, A., High, K. A., Austin, R. C., and Kruger, W. D. (2009) *FASEB J.* **23,** 883–893
60. Starcher, B., and Hill, C. H. (2005) *Exp. Lung Res.* **31,** 873–885